

Search for CP Violations in the Production and Decay of the Hyperon-Antihyperon Pairs

Mengjiao Guo,^{1,*} Zhe Zhang,^{2,†} Ronggang Ping,^{3,4,‡} and Jianbin Jiao^{1,§}

¹*Institute of Frontier and Interdisciplinary Science, Shandong University, Qingdao 266237, China*

²*Southern Center for Nuclear-Science Theory (SCNT), Institute of Modern Physics, Chinese Academy of Sciences, Huizhou 516000, China*

³*Institute of High Energy Physics, Chinese Academy of Sciences, Beijing 100049, China*

⁴*University of Chinese Academy of Sciences, Beijing 100049, China*

(Dated: February 28, 2025)

This study introduces a novel joint angular distribution analysis for the process $e^+e^- \rightarrow J/\psi \rightarrow B(\rightarrow B_1\pi)\bar{B}(\rightarrow \bar{B}_1\pi)$, where B and B_1 are hyperons. We consider both transverse and longitudinal beam polarization and analyze CP violation in the production and decay of hyperons. We present the complete Hessian matrix for the sensitivities of the weak decay parameters α_- , α_+ , ϕ_Ξ and $\bar{\phi}_\Xi$, the P-violating term F_A , and the EDM d_B (derived from the CP-violating term H_T), under the BESIII and STCF statistics. We find that polarization enhances the sensitivity of the parameters. Specifically, longitudinal polarization provides a more significant improvement compared to transverse polarization, with the enhancement being more pronounced for single-step decays than for multi-step decays. With the expected statistics from the BESIII experiment, the estimated EDM sensitivities for Λ and Σ^+ are on the order of 10^{-19} e cm, while those for Ξ^- and Ξ^0 are 10^{-18} e cm. Furthermore, the STCF experiment is expected to improve these estimates by $1 \sim 2$ orders of magnitude. For hyperon decay parameters, a 1σ measurement of A_{CP} can be achieved at BESIII, while at STCF, A_{CP} can be observed with a significance exceeding 10σ .

I. INTRODUCTION

If matter and antimatter were created in equal amounts during the Big Bang [1–3], the observed universe's dominance by ordinary matter, with antimatter being extremely rare, remains a profound puzzle. In 1967, A.D. Sakharov [4] proposed three essential conditions for generating an asymmetry between matter and antimatter, one of which is the charge conjugation (C) violation and the combined violation of C and parity (P) symmetries, known as CP violation. CP violation was first observed in neutral K mesons decay [5], and later in B [6, 7] and D [8] mesons.

Within the Standard Model, CP violation is governed by two main parameters: the complex phase in the Cabibbo-Kobayashi-Maskawa (CKM) matrix [9, 10], which influences weak interactions, and the Quantum Chromodynamics (QCD) angle θ [11], which relates to CP violation in strong interactions. The experimental upper bound on the neutron electric dipole moment (EDM) constrains the strong CP-violating parameter $\bar{\theta}$ to be less than 10^{-10} [11–13]. This indicates that strong CP violation is dynamically suppressed within the Standard Model, a phenomenon known as the strong CP problem [14–16]. While experimental research on CP violation has aligned with the predictions of the Standard Model, the observed degree

of CP violation is insufficient to fully account for the matter-antimatter asymmetry in the universe.

The search for new physics through CP violation in hyperon production processes has become a promising research direction. In hyperon production, the primary source of CP violation is the EDM. In a magnetic field \vec{B} and electric field \vec{E} , a particle's Hamiltonian can be represented as [17–19]:

$$\mathcal{H} = -\vec{\mu} \cdot \vec{B} - \vec{d} \cdot \vec{E}. \quad (1)$$

Here, \vec{d} and $\vec{\mu}$ denote the EDM and magnetic dipole moment of the particle, respectively. The EDM is a function of charge distribution, $\rho(\vec{r})$, defined as $\vec{d} = \int \vec{r} \rho(\vec{r}) d^3r$ and quantifying the electric charge separation. Fig. 1 illustrates the effect of P and time-reversal (T) transformations on a particle with EDM. The EDM of a system \vec{d} must be parallel (or antiparallel) to the average angular momentum of system \vec{J} . The magnetic field \vec{B} and the angular momentum operator \vec{J} are both even under P but odd under T, while the electric field \vec{E} is odd under P but even under T. Thus, under the constraint of CPT conservation [20, 21], the existence of $\vec{d} \neq 0$ implies C and CP violations.

Since the 1950s, EDM search efforts have yielded constraints on the EDMs of various particles, including leptons [22–32], neutrons [33–36], heavy atoms [37–40], and protons [41–43]. For hyperons, only the EDM of the Λ , has been measured, with a precision of $|d_\Lambda| < 1.5 \times 10^{-16}$ e cm (95% C.L.) at Fermilab [44]. This value is significantly larger than that for nucleons, while theoretical estimates based on neutron EDMs predict an upper

* guomj@mail.sdu.edu.cn

† zhangzhe@impcas.ac.cn

‡ pingrg@ihep.ac.cn

§ jiaojb@sdu.edu.cn

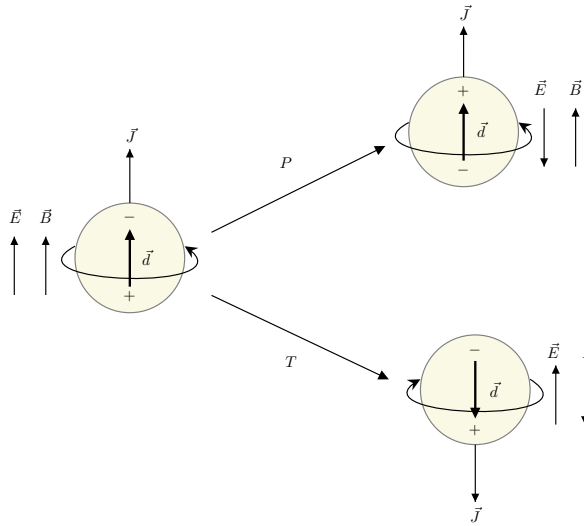


FIG. 1: Transformations of a spin- s particle under P and T operators, along with the particle's electric dipole moment (\vec{d}), and the external magnetic (\vec{B}) and electric (\vec{E}) fields. A permanent electric dipole moment \vec{d} of a fundamental particle is proportional to its angular momentum \vec{J} . It shows that the invariance of the particle dipole moment under P and T transformations is maintained only when $\vec{d} = 0$.

limit of about $4.4 \times 10^{-26} e \text{ cm}$ [45–48].

In the decay processes of hyperons, CP violation can be investigated through the decay parameters. The decay amplitude of a spin-1/2 hyperon into a lighter spin-1/2 baryon and a pseudoscalar meson consists of both a P-violating S-wave component and a P-conserving P-wave component. Consequently, this process can be fully described by two independent decay parameters, α and ϕ [49–51]. According to CP symmetry, the decay parameters α and ϕ should exhibit opposite signs. For hyperons with multiple strange quarks, the CKM mechanism in the Standard Model predicts very low CP asymmetry values, between $10^{-5} \sim 10^{-4}$ [52]. This suggests hyperons are particularly sensitive to CP-violating effects beyond the Standard Model, highlighting their importance as probes for new physics.

The process of e^+e^- annihilation generates spin-entangled hyperon-antihyperon pairs, offering a unique opportunity to study CP violation in the production and decay processes of hyperons [53–63]. BESIII [64, 65] has collected the world's largest J/ψ dataset [66] and provided the most precise measurements to date of CP violation in hyperon decay processes [67–76]. Theoretical discussions on the EDM of this process have also gradually commenced [77, 78], while the impact of beam polarization on experimental measurements has garnered significant interest [56, 79–84]. The proposed Super Tau-Charm Factory (STCF) is expected to increase the J/ψ statistics by two orders of magnitude [85], offering new opportunities

to explore CP violation in hyperon-related processes.

In this paper, we present a systematic analysis of CP violation in the production and decay processes of hyperons under conditions where the beam possesses both transverse and longitudinal polarization. For the $e^+e^- \rightarrow J/\psi$ decay, we investigate the influence of beam polarization on the polarization of J/ψ and present its complete spin density matrix (SDM). For the $J/\psi \rightarrow B\bar{B}$ (B denotes a hyperon) decay, we provide the production density matrix of hyperons, including the CP-violating term H_T and the P-violating term F_A . We establish the relationship between H_T , F_A , and the EDM of hyperons as well as weak coupling angles. Regarding the decay processes of hyperons, we focus on Λ , Σ^+ , Ξ^- and Ξ^0 hyperons, and present their decay density matrices. Using the decay parameters of hyperons, we define two parameters, A_{CP} and B_{CP} , to characterize CP violation. These parameters are related to the strong and weak phase angles in the decay processes. Finally, we express the joint angular distribution of all products in terms of the production and decay SDMs of hyperons.

We estimate the sensitivity to CP violation by constructing the Hessian matrix of the joint angular distribution. Under the BESIII and the proposed STCF statistics, we compare the sensitivity of different hyperon EDMs and decay parameters for non-polarized beams, 80% transversely polarized beams, and 80% longitudinally polarized beams. We also discuss the comparison of CP violation sensitivity with existing experimental and theoretical results.

This paper is organized as follows. In Sec. II, we provide the analysis of CP violations for the production and decay of the hyperons and the joint angular distribution for these processes. In Sec. III, we derive the statistical sensitivity of CP violations. A summary is given in Sec. IV.

II. PRODUCTION AND DECAY CHAINS OF HYPERONS

The process $e^+e^- \rightarrow J/\psi \rightarrow B\bar{B}$ serves as a crucial tool for studying the properties of hyperons. In this chapter, we discuss CP violation in this reactions and present the joint angular distributions of all final particles.

A. J/ψ polarization with polarized beams

A suitable way is to give the density matrices of electron and positron in their helicity rest frames S_A , S_B , reached from the center-of-mass(c.m.) of the reactions as shown in Fig. 2.

In certain experimental facilities, such as the proposed STCF, longitudinally polarized beams can be prepared, with the longitudinal polarization denoted as P_L . Additionally, synchrotron radiation aligns the spins of positrons and electrons either parallel or antiparallel to the magnetic field direction, respectively, leading to transverse

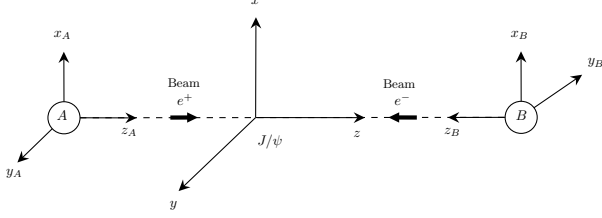


FIG. 2: Helicity rest frames for electron and positron beams and that for the J/ψ meson in the c.m. frame.

polarizations denoted as P_T . In an electron-positron annihilation experiment with symmetric beam energy, the Sokolov-Ternov effect [86] requires equal degrees of transverse polarization.

Consequently, the SDM of the leptons is represented in their helicity frame as follows:

$$\begin{aligned} \rho^- &= \frac{1}{2} \begin{pmatrix} 1 + P_L & P_T \\ P_T^* & 1 - P_L \end{pmatrix} \text{ for } e^-, \\ \rho^+ &= \frac{1}{2} \begin{pmatrix} 1 + \bar{P}_L & P_T \\ P_T^* & 1 - \bar{P}_L \end{pmatrix} \text{ for } e^+, \end{aligned} \quad (2)$$

taking into account both longitudinal and transverse components of the polarization vectors. In the laboratory system, the SDM element of J/ψ in the $e^+e^- \rightarrow J/\psi$ decay is expressed as:

$$\begin{aligned} \rho_{\lambda,\lambda'}^{J/\psi} &= \sum_{\lambda_-, \lambda'_-, \lambda_+, \lambda'_+} D_{\lambda, \lambda_+ - \lambda_-}^{1*}(0, 0, 0) D_{\lambda'_+, \lambda'_+ - \lambda'_-}^1(0, 0, 0) \\ &\times \rho_{\lambda_+, \lambda'_+}^+ \rho_{\lambda_-, \lambda'_-}^- \delta_{\lambda_+, -\lambda_-} \delta_{\lambda'_+, -\lambda'_-}, \end{aligned} \quad (3)$$

where $\lambda_+^{(')}, \lambda_-^{(')}$ represent the helicities of the positron and electron, and $D_{\lambda, \lambda'}^j(0, 0, 0)$ is the Wigner D -matrix. The Dirac δ -function in the above equation ensures the conservation of helicity during the electron-positron annihilation process.

B. CP violation in hyperon-antihyperon pairs production

Hyperon-antihyperon pairs produced in J/ψ decays are spin-entangled. The production density matrix R can be calculated as:

$$\begin{aligned} R_{\lambda_1, \lambda_2, \lambda'_1, \lambda'_2} &\propto \sum_{\lambda, \lambda'} \rho_{\lambda, \lambda'}^{J/\psi} D_{\lambda, \lambda_1 - \lambda_2}^{1*}(\theta, \phi) \\ &\times D_{\lambda'_1, \lambda'_1 - \lambda'_2}^1(\theta, \phi) \mathcal{A}_{\lambda_1, \lambda_2} \mathcal{A}_{\lambda'_1, \lambda'_2}^*. \end{aligned} \quad (4)$$

Here, λ_1 and λ_2 represent the helicities of the hyperons and their antiparticles. The helicity amplitudes $\mathcal{A}_{\lambda_1, \lambda_2}$ characterize the decay process $J/\psi \rightarrow B\bar{B}$, and the angles θ and ϕ denote the hyperon's momentum direction in the J/ψ helicity rest frame. The helicities of

the produced hyperons can take the values $(\lambda_1, \lambda_2) = (\pm 1/2, \pm 1/2)$, with polarization effects encoded in the SDM. The matrix R thus provides a critical framework for studying polarization-dependent observables in hyperon-antihyperon pairs.

The general form of the helicity amplitude for the decay process $J/\psi \rightarrow B\bar{B}$ is defined as [77, 87]

$$\begin{aligned} \mathcal{A}_{\lambda_1, \lambda_2} &= \epsilon_\mu(\lambda_1 - \lambda_2) \bar{u}(\lambda_1, p_1)(F_V \gamma^\mu + \frac{i}{2m} \sigma^{\mu\nu} q_\nu H_\sigma \\ &+ \gamma^\mu \gamma^5 F_A + \sigma^{\mu\nu} \gamma^5 q_\nu H_T) \nu(\lambda_2, p_2). \end{aligned} \quad (5)$$

Here, m is the mass of the B hyperon, and p_1 and p_2 represent the four momentum of B and \bar{B} , respectively, and ϵ_μ is the polarization vector of J/ψ . The form factors F_V and H_σ correspond to the Dirac and Pauli terms, while F_A and H_T capture P-violating and CP-violating terms, respectively.

The magnetic and electric form factors G_1 and G_2 are defined as [88, 89]:

$$G_1 = F_V + H_\sigma, \quad G_2 = G_1 - \frac{(p_1 - p_2)^2}{4m^2} H_\sigma. \quad (6)$$

The angular asymmetry parameters $\alpha_{J/\psi}$ and $\Delta\Phi$ are related to these form factors as follows:

$$\alpha_{J/\psi} = \frac{M_{J/\psi}^2 |G_1|^2 - 4m^2 |G_2|^2}{M_{J/\psi}^2 |G_1|^2 + 4m^2 |G_2|^2}, \quad (7)$$

$$\frac{G_1}{G_2} = \left| \frac{G_1}{G_2} \right| e^{-i\Delta\Phi}. \quad (8)$$

The P-violating term F_A , primarily arising from Z -boson exchange, is related to the weak mixing angle θ_W as:

$$F_A \approx -\frac{1}{6} D g_V \frac{g^2}{4 \cos^2 \theta_W} \frac{1 - 8 \sin^2 \theta_W / 3}{m_Z^2}, \quad (9)$$

where $g = e / \sin \theta_W$ is the gauge coupling constants with $e = \sqrt{4\pi/137}$, $D = 0.8$ is a weighted coupling constant in the light quark flavor SU(3) limit and $g_V = 1.35$ GeV represents the coupling strength between charm quark currents and the J/ψ . Then, the expected P-violating effect is approximately -1.07×10^{-6} [77].

The CP-violating term H_T is linked to the EDM of the hyperon through [77, 87, 90]:

$$H_T = \frac{2e}{3M_{J/\psi}^2} g_V d_B. \quad (10)$$

It is worth mentioning that both F_A and H_T are complex in the timelike region. A straightforward parameterization scheme is:

$$F_A = |F_A| e^{i\phi_A}, \quad (11)$$

$$H_T = |H_T| e^{i\phi_T}. \quad (12)$$

In the following sections, I will use the magnitude of the EDM in the timelike region, $|d_B|$, as a reference for comparison with the hadronic EDM in the spacelike region..

Due to the smallness of P and CP violation, contributions from the F_A and H_T terms to the decay width of J/ψ can be safely neglected such that [78]

$$\Gamma_{J/\psi \rightarrow B\bar{B}} = \frac{|G_1|^2 M_{J/\psi}}{12\pi} \sqrt{1 - \frac{4m^2}{M_{J/\psi}^2}} \left(1 + \frac{2m^2}{M_{J/\psi}^2}\right) \left|\frac{G_2}{G_1}\right|^2. \quad (13)$$

When considering P and CP violation effects, along with the longitudinal and transverse polarization of the beams, the production SDM R for the $B\bar{B}$ hyperon pair are described in Appendix A.

C. CP violation in hyperon decays

Due to their short lifetimes, hyperons decay into more stable particles, such as baryons (B_1) and mesons, through weak interactions. The weak decay severs as the spin self-analyzer. The decay SDM, T , for a hyperon decaying into a baryon and a meson is given by:

$$T_{\lambda_1, \lambda_3, \lambda'_1, \lambda'_3} \propto D_{\lambda_1, \lambda_3}^{1/2}(\theta, \phi) D_{\lambda'_1, \lambda'_3}^{*1/2}(\theta, \phi) A_{\lambda_3} A_{\lambda'_3}^*, \quad (14)$$

where λ_1 represents the helicity of the hyperon and λ_3 represents the helicity of the baryon in the decay products. The angles θ and ϕ are the polar and azimuthal angles of the produced baryon in the hyperon rest frame. A_λ denotes the helicity amplitude of this decay process and can be parametrized as

$$\alpha_D = |A_{1/2}|^2 - |A_{-1/2}|^2 = 2\text{Re}(A_S^* A_P), \quad (15)$$

$$\beta_D = 2\text{Im}[A_{1/2} A_{-1/2}^*] = 2\text{Im}(A_S^* A_P), \quad (16)$$

$$\gamma_D = 2\text{Re}[A_{1/2} A_{-1/2}^*] = |A_S|^2 - |A_P|^2, \quad (17)$$

where $\beta_D = \sqrt{1 - \alpha_D^2} \sin \phi_D$ and $\gamma_D = \sqrt{1 - \alpha_D^2} \cos \phi_D$. With this parametrization scheme, the specifics of the decay SDM can be found in Appendix B.

The P-violating S-wave component and a P-conserving P-wave component can be expressed as follows [51]:

$$A_S = \sum_{i,j} S_{i,j} e^{i(\delta_j^S + \phi_{i,j}^S)}, \quad (18)$$

$$A_P = \sum_{i,j} P_{i,j} e^{i(\delta_j^P + \phi_{i,j}^P)}. \quad (19)$$

Here, $S_{i,j}$ and $P_{i,j}$ are real-valued, with $\{i, j\} = \{\Delta I, I\}$ indexing all possible weak isospin transitions and final

state isospins . The phase δ_i represents the phase shift due to strong final-state interactions, while $\phi_{i,j}$ denotes the CP violation phase arising from weak interactions. For the conjugate process, we have

$$\bar{A}_S = - \sum_{i,j} S_{i,j} e^{i(\delta_i^S - \phi_{i,j}^S)}, \quad (20)$$

$$\bar{A}_P = \sum_{i,j} P_{i,j} e^{i(\delta_i^P - \phi_{i,j}^P)}. \quad (21)$$

In the CP conservation limit, the amplitudes \bar{A}_S and \bar{A}_P for the charge-conjugated decay mode of the antibaryon \bar{D} are $\bar{A}_S = -A_S$ and $\bar{A}_P = A_P$. Therefore, the decay parameters have the opposite values: $\alpha_D = -\bar{\alpha}_D$ and $\beta_D = -\bar{\beta}_D$. Two independent experimental CP violation tests can be defined using these observables,

$$A_{CP} := \frac{\alpha_D + \bar{\alpha}_D}{\alpha_D - \bar{\alpha}_D}, \quad (22)$$

$$B_{CP} := \frac{\beta_D + \bar{\beta}_D}{\alpha_D - \bar{\alpha}_D}. \quad (23)$$

If one works to leading order in the decay parameters α_D and ϕ_D , B_{CP} can also be expressed as

$$B_{CP} = \Phi_{CP} \frac{\sqrt{1 - \langle \alpha_D \rangle^2}}{\langle \alpha_D \rangle} \cos \langle \phi_D \rangle - A_{CP} \frac{\langle \alpha_D \rangle}{1 - \langle \alpha_D \rangle^2} \sin \langle \phi_D \rangle. \quad (24)$$

The hyperon-antihyperon average value is defined as

$$\langle \alpha_D \rangle = \frac{\alpha_D - \bar{\alpha}_D}{2}, \quad \langle \phi_D \rangle = \frac{\phi_D - \bar{\phi}_D}{2} \quad (25)$$

and

$$\Phi_{CP} := \frac{\phi_D + \bar{\phi}_D}{2} \quad (26)$$

is based on the spin-rotation decay parameter ϕ_D .

For convenience, we construct a strong-phase related observable

$$\Delta C = \frac{\beta - \bar{\beta}}{\alpha - \bar{\alpha}}. \quad (27)$$

The correspondence between these observables and the strong and weak phase angles is listed in Appendix C.

It should be noted that in some experimental measurement studies, the contributions from the higher-isospin transition partial waves are omitted when presenting the measured values of the strong and weak phases. This approach is not entirely accurate. Such as, for Ξ^- hyperon, in the first order in the $\Delta I = \frac{3}{2}$ amplitudes and the weak-interaction phases, we find

$$A_{CP} = -\tan(\delta_2^P - \delta_2^S) \tan(\phi_{12}^P - \phi_{12}^S) \left[1 + \frac{1}{2} \frac{S_{32}}{S_{12}} \left(\frac{\sin(\phi_{12}^P - \phi_{32}^S)}{\sin(\phi_{12}^P - \phi_{12}^S)} - 1 \right) + \frac{1}{2} \frac{P_{32}}{P_{12}} \left(\frac{\sin(\phi_{32}^P - \phi_{12}^S)}{\sin(\phi_{12}^P - \phi_{12}^S)} - 1 \right) + \frac{1}{4} \frac{S_{32}P_{32}}{S_{12}P_{12}} \left(\frac{\sin(\phi_{32}^P - \phi_{32}^S)}{\sin(\phi_{12}^P - \phi_{12}^S)} - 1 \right) \right], \quad (28)$$

$$B_{CP} = \tan(\phi_{12}^P - \phi_{12}^S) \left[1 + \frac{1}{2} \frac{S_{32}}{S_{12}} \left(\frac{\sin(\phi_{12}^P - \phi_{32}^S)}{\sin(\phi_{12}^P - \phi_{12}^S)} - 1 \right) + \frac{1}{2} \frac{P_{32}}{P_{12}} \left(\frac{\sin(\phi_{32}^P - \phi_{12}^S)}{\sin(\phi_{12}^P - \phi_{12}^S)} - 1 \right) + \frac{1}{4} \frac{S_{32}P_{32}}{S_{12}P_{12}} \left(\frac{\sin(\phi_{32}^P - \phi_{32}^S)}{\sin(\phi_{12}^P - \phi_{12}^S)} - 1 \right) \right], \quad (29)$$

$$\Delta C = \tan(\delta_2^P - \delta_2^S). \quad (30)$$

Generally, one believes that $\Delta I = \frac{3}{2}$ amplitudes are much smaller than $\Delta I = \frac{1}{2}$ amplitudes. However, recent measurements of Λ decay [91] have posed significant challenges to this understanding. Additionally, in the above equations, the ratios between phase differences of varied isospin transition partial waves are involved, and our knowledge of these phases remains limited. This could potentially enhance the contribution of higher isospin transition ΔI amplitudes. For accurate measurements of the strong and weak phases, we recommend determining them through a joint fit of decay processes involving particles with different isospin states, such as the joint fit of Ξ^- and Ξ^0 .

D. Joint angular distribution in hyperon production and decay

For the productions and decays of Λ or Σ pairs, they undergo only single-step decay chains, such as $\Lambda \rightarrow p\pi^-$ or $\Sigma^+ \rightarrow p\pi^0$. The joint angular distribution of all final products can be expressed as

$$\begin{aligned} \frac{d\sigma}{d\Omega} &\propto \mathcal{W}(\boldsymbol{\eta}; \boldsymbol{\omega}) \\ &= \sum_{[\lambda]} R_{\lambda_1, \lambda_2, \lambda'_1, \lambda'_2} T_{\lambda_1, \lambda_3, \lambda'_1, \lambda_3} T_{\lambda_2, \lambda_4, \lambda'_2, \lambda_4}. \end{aligned} \quad (31)$$

The set $[\lambda]$ in the given expression encompasses all helicity symbols participating in the summation, and others.

For the productions and decays of Ξ^- or Ξ^0 pairs, they undergo two-step decay chains, such as $\Xi^{-(0)} \rightarrow \Lambda\pi^{-(0)}$ followed by $\Lambda \rightarrow p\pi^-$. The joint angular distribution of all products can be expressed as

$$\begin{aligned} \frac{d\sigma}{d\Omega} &\propto \mathcal{W} \\ &= \sum_{[\lambda]} R_{\lambda_1, \lambda_2, \lambda'_1, \lambda'_2} \\ &\times T_{\lambda_1, \lambda_3, \lambda'_1, \lambda'_3} T_{\lambda_2, \lambda_4, \lambda'_2, \lambda'_4} T_{\lambda_3, \lambda_5, \lambda'_3, \lambda_5} T_{\lambda_4, \lambda_6, \lambda'_4, \lambda_6}. \end{aligned} \quad (32)$$

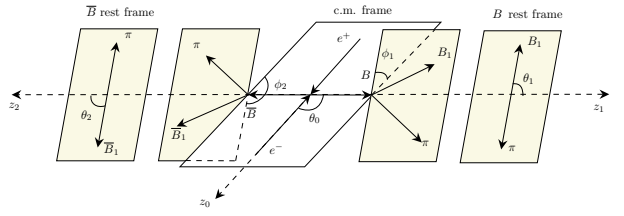


FIG. 3: Helicity angles in single-step decays, such as $J/\psi \rightarrow B(\rightarrow B_1\pi)\bar{B}(\rightarrow \bar{B}_1\pi)$ decays, where B represents a Λ or Σ^+ hyperon.

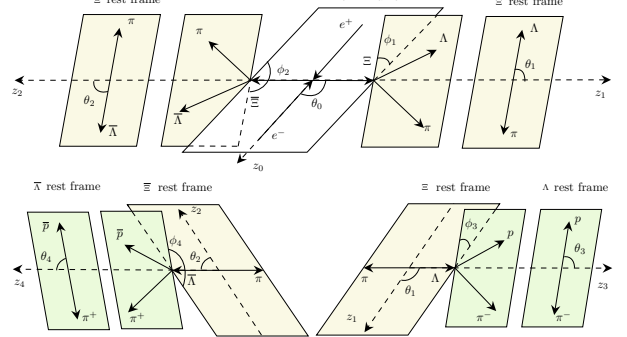


FIG. 4: Helicity angles in two-step decays, such as $J/\psi \rightarrow B(\rightarrow B_1\pi)\bar{B}(\rightarrow \bar{B}_1\pi)$ decays, where B represents a Ξ^0 or Ξ^- hyperon.

Figs. 3 and 4 illustrate the helicity angles within the corresponding helicity frame for single-step and two-step decays, respectively.

III. STATISTICAL SIGNIFICANCE

To assess the sensitivity of the production and decay parameters of hyperons to experimental statistics, we constructed a Hessian matrix of these parameters, explicitly accounting for their correlation matrix elements. The

joint angular distribution \mathcal{W} is normalized as follows:

$$\tilde{\mathcal{W}} = \frac{\mathcal{W}(\boldsymbol{\eta})}{\int \mathcal{W}(\boldsymbol{\eta}) d\boldsymbol{\eta}}, \quad (33)$$

where $\boldsymbol{\eta} = (\theta, \phi, \theta_1, \phi_1, \theta_2, \phi_2, \theta_3, \phi_3, \theta_4, \phi_4)$ represents the polar and azimuthal angles of all products. The likelihood function for the observed data is defined as:

$$L(\boldsymbol{\eta} | \boldsymbol{\omega}) = \prod_{i=1}^n \tilde{\mathcal{W}}_i, \quad (34)$$

where n is the total number of events, and $\boldsymbol{\omega}$ represents the hyperon production and decay parameters. Under the assumptions of the likelihood function satisfies the regularity conditions and the polar angles and azimuthal angles are independent of the parameter $\boldsymbol{\omega}$, the Hessian matrix element of the maximum likelihood estimate is given as [92]

$$V_{ij}^{-1}(\boldsymbol{\omega}_i) = n \int \frac{1}{\tilde{\mathcal{W}}} \left(\frac{\partial \tilde{\mathcal{W}}}{\partial \omega_i} \right) \left(\frac{\partial \tilde{\mathcal{W}}}{\partial \omega_j} \right) d\boldsymbol{\eta}, \\ i, j = 1, 2, \dots, k, \quad (35)$$

where k is the number of parameters. It is worth noting that the inversion here is performed on the entire matrix. Then, the standard error for ω_i is computed as:

$$\delta(\omega_i) = \sqrt{V_{ii}}. \quad (36)$$

For Λ and Σ^+ , only the single-step decay angles $\theta_1(\theta_2)$ and $\phi_1(\phi_2)$ are relevant. While for Ξ^- and Ξ^0 , the second-step decay angular variables $\theta_3(\theta_4)$ and $\phi_3(\phi_4)$ are also incorporated. The hyperon parameter measurements are summarized in Table I, and the estimated hyperon statistics collected by BESIII and STCF are shown in Table II.

Under the BESIII and STCF statistics, we display the sensitivities for the weak decay parameters α_- , α_+ , ϕ_Ξ and $\bar{\phi}_\Xi$ (only for Ξ^- and Ξ^0), the P-violating form factor F_A and the EDM derived from the CP-violating term H_T in Table III. In our calculations, we compared the sensitivity of various parameters for unpolarized, 80% transversely polarized, and 80% longitudinally polarized beams. The dependence of hyperon decay parameters on event statistics is detailed in Appendix D.

While the BESIII beam is generally assumed to have no longitudinal polarization, recent theoretical studies suggest possible transverse polarization, though its magnitude remains unmeasured. In contrast, the STCF explicitly proposes a longitudinally polarized beam [85]. Thus, sensitivity predictions for BESIII are more reliable for the unpolarized scenario, while for STCF, the longitudinally polarized scenario is more relevant. As shown in Table III, with the same statistics, polarization significantly enhances sensitivity more for single-step decays than for multi-step decays, and longitudinal polarization offers a much greater improvement compared to transverse polarization. This observation could provide valuable guidance for future accelerator designs.

Under BESIII statistics, the EDM sensitivities for Λ and Σ^+ are expected to reach approximately $10^{-19} e \text{ cm}$, with the Λ EDM measurement representing a three-order-of-magnitude improvement compared to the Fermilab result [44]. For Ξ^- and Ξ^0 hyperons, the EDM sensitivities are estimated to be $10^{-18} e \text{ cm}$. The STCF experiment, with its higher luminosity and broader energy range, is expected to improve EDM sensitivities by $1 \sim 2$ orders of magnitude, further advancing the search for new physics. While this remains below the theoretical expectation for the hyperon EDM of $\mathcal{O}(10^{-26})$ [48], it could still provide a significant avenue for exploring new physics.

For hyperon decay parameters, BESIII achieves a sensitivity of $\mathcal{O}(10^{-3})$, whereas STCF is expected to reach $\mathcal{O}(10^{-4})$, approaching the theoretical upper limit for CP violation in hyperons, predicted to be $\mathcal{O}(10^{-5} \sim 10^{-4})$ [50, 51]. Table IV summarizes the CP-violating observables A_{CP} and $\Delta\Phi_{CP}$, indicating that future STCF experiments could observe CP violation at the 17σ level.

IV. SUMMARY

This paper systematically analyzes P and CP violation in the production and decay of hyperons in the process $e^+e^- \rightarrow J/\psi \rightarrow B(\rightarrow B_1\pi)\bar{B}(\rightarrow B_1\pi)$. We study the effects of transversely and longitudinally polarized beams on J/ψ polarization. For $J/\psi \rightarrow B\bar{B}$ decay, we derive the decay amplitude including the P-violating term F_A and CP-violating term H_T , and analyze their relations to the weak coupling angle and the hyperon EDM. We derive the production density matrix for hyperon production. For hyperon decays, we express the decay density matrix in terms of decay parameters and define two CP-violating observables, A_{CP} and B_{CP} . Finally, we present the joint angular distribution for hyperon production and decay processes.

Using Hessian matrix analysis, we estimate the sensitivity of hyperon parameters under BESIII and STCF statistics. The results show that polarization significantly enhances sensitivity for single-step decays compared to multi-step decays, with longitudinal polarization providing a much larger improvement than transverse polarization. Under BESIII statistics, the sensitivity of the hyperon EDM is $\mathcal{O}(10^{-18})$, while STCF could reach $\mathcal{O}(10^{-20})$. For hyperon decays, proposed STCF experiments may observe evidence of CP violation at the 17σ level.

This work provides a theoretical framework for CP violation studies and new physics searches using polarized beams at BESIII and proposed STCF, while offering valuable insights for the design and construction of STCF.

ACKNOWLEDGMENTS

The authors thank Liang Yan, Yong Du, Jianyu Zhang, Shengliang Hu, Shaojie Wang for useful discussions.

TABLE I: Measured values of decay parameters for $e^+e^- \rightarrow J/\psi \rightarrow B\bar{B}$, with final states listed in the first row and G_1 and G_2 calculated from $\alpha_{J/\psi}$ and $\Delta\Phi$.

Decay channel	$J/\psi \rightarrow \Lambda\bar{\Lambda}$ [67]	$J/\psi \rightarrow \Sigma^+\bar{\Sigma}^-$ [70]	$J/\psi \rightarrow \Xi^-\bar{\Xi}^+$ [72]	$J/\psi \rightarrow \Xi^0\bar{\Xi}^0$ [73]
\sqrt{s} (GeV)	$M_{J/\psi}$	$M_{J/\psi}$	$M_{J/\psi}$	$M_{J/\psi}$
$\alpha_{J/\psi}^B$	0.4748	-0.508	0.586	0.514
α_-	0.7519	-0.998	-0.376	-0.375
α_+	-0.7559	0.990	0.371	0.379
ϕ_Ξ (rad)	-	-	0.011	0.0051
$\bar{\phi}_\Xi$ (rad)	-	-	-0.021	-0.0053
$\Delta\Phi$ (rad)	0.7521	-0.270	1.213	1.168
$G_1 (\times 10^{-3})$	1.61	0.86	1.36	1.47
$G_2 (\times 10^{-3})$	$0.97 + 0.91i$	$1.89 - 0.52i$	$0.29 + 0.76i$	$0.38 + 0.90i$

This work is supported by the National Natural Science Foundation of China (NSFC) under Grants Nos. 12447132, 12175244, 12375070, 12475082, the Natural Science Foundation of Shan-dong Province under Contract

No. ZR2023MA004, the National Key R&D Program of China under Contracts No. 2020YFA0406300, the Joint LargeScale Scientific Facility Funds of the NSFC and CAS under Contract No. U1832207.

Appendix A: Production SDM of hyperon antihyperon pairs

When considering P and CP violation effects, as well as the longitudinal and transverse polarization, the production SDM R for the hyperon-antihyperon pair can be expressed as:

$$\begin{aligned}
R_{++++} = & 2 \sin^2 \theta (1 - P_T^2 \cos 2\phi) [m^2 |F_V|^2 + \frac{E_c^4}{m^2} |H_\sigma|^2 \\
& - 4m^2 E_c^2 |H_T|^2 + 4E_c^4 |H_T|^2 + 2E_c^2 \text{Re}[F_V H_\sigma^*] + 4mE_c \sqrt{E_c^2 - m^2} \text{Im}[F_V H_T^*] + \frac{4E_c^3 \sqrt{E_c^2 - m^2}}{m} \text{Im}[H_\sigma H_T^*]], \\
R_{-+++} = & 2 \sin \theta [\cos \theta + P_L - P_T^2 (\cos \theta \cos 2\phi - i \sin 2\phi)] \\
& \times [mE_c |F_V|^2 + \frac{E_c^3}{m} |H_\sigma|^2 + mE_c H_\sigma F_V^* + \frac{E_c^3}{m} F_V H_\sigma^* - m \sqrt{E_c^2 - m^2} F_A F_V^* \\
& - 2iE_c^2 \sqrt{E_c^2 - m^2} F_V H_T^* - 2iE_c^2 \sqrt{E_c^2 - m^2} H_\sigma H_T^* - \frac{E_c^2 \sqrt{E_c^2 - m^2}}{m} F_A H_\sigma^* + 2iE_c (E_c^2 - m^2) F_A H_T^*], \\
R_{+-++} = & 2 \sin \theta [\cos \theta - P_L - P_T^2 (\cos \theta \cos 2\phi + i \sin 2\phi)] \\
& \times [-mE_c |F_V|^2 - \frac{E_c^3}{m} |H_\sigma|^2 - \frac{E_c^3}{m} F_V H_\sigma^* - mE_c H_\sigma F_V^* - m \sqrt{E_c^2 - m^2} F_A F_V^* \\
& - \frac{E_c^2 \sqrt{E_c^2 - m^2}}{m} F_A H_\sigma^* + 2iE_c^2 \sqrt{E_c^2 - m^2} F_V H_T^* + 2iE_c^2 \sqrt{E_c^2 - m^2} H_\sigma H_T^* + 2iE_c (E_c^2 - m^2) F_A H_T^*], \\
R_{+-+-} = & 2 \sin \theta [\cos \theta + P_L - P_T^2 (\cos \theta \cos 2\phi + i \sin 2\phi)] \\
& \times [mE_c |F_V|^2 + \frac{E_c^3}{m} |H_\sigma|^2 + mE_c F_V H_\sigma^* + \frac{E_c^3}{m} H_\sigma F_V^* - m \sqrt{E_c^2 - m^2} F_V F_A^* \\
& - \frac{E_c^2 \sqrt{E_c^2 - m^2}}{m} H_\sigma F_A^* + 2iE_c^2 \sqrt{E_c^2 - m^2} H_T F_V^* + 2iE_c^2 \sqrt{E_c^2 - m^2} H_T H_\sigma^* - 2iE_c (E_c^2 - m^2) H_T F_A^*], \\
R_{+++-} = & 2 \sin \theta [\cos \theta - P_L - P_T^2 (\cos \theta \cos 2\phi - i \sin 2\phi)] \\
& \times [-mE_c |F_V|^2 - \frac{E_c^3}{m} |H_\sigma|^2 - mE_c F_V H_\sigma^* - \frac{E_c^3}{m} H_\sigma F_V^* - m \sqrt{E_c^2 - m^2} F_V F_A^*
\end{aligned}$$

TABLE II: Estimated yields of pseudoexperiments based on the statistics from BESIII and STCF experiments, where B_{tag} represents the branching ratio of cascade decay, ϵ_{tag} represents the expected detection efficiency, and N_{tag}^{evt} represents the number of expected events after reconstruction.

Decay channel	$J/\psi \rightarrow \Lambda\bar{\Lambda}$	$J/\psi \rightarrow \Sigma^+\bar{\Sigma}^-$	$J/\psi \rightarrow \Xi^-\bar{\Xi}^+$	$J/\psi \rightarrow \Xi^0\bar{\Xi}^0$
$B_{tag}/(\times 10^{-4})$ [93]	7.77	2.78	3.98	4.65
$\epsilon/\%$ [67, 70, 72, 73]	40	25	15	7
$N_{tag}^{evt}/(\times 10^5)$ (BESIII) [67, 70, 72, 73]	31.3	7.0	6.0	3.3
$N_{tag}^{evt}/(\times 10^8)$ (STCF) [85]	10.6	2.4	2.0	1.1

TABLE III: Estimated sensitivities for the weak decay parameters α_- , α_+ , ϕ_Ξ , and $\bar{\phi}_\Xi$, the P-violating term F_A , and the electric dipole moment d_B , based on the statistics collected by BESIII and STCF. The table presents, from top to bottom, the achievable sensitivities in each experiment without polarization, with the addition of 80% longitudinal polarization, and with the addition of 80% transverse polarization.

	$J/\psi \rightarrow \Lambda\bar{\Lambda}$		$J/\psi \rightarrow \Sigma^+\bar{\Sigma}^-$		$J/\psi \rightarrow \Xi^-\bar{\Xi}^+$		$J/\psi \rightarrow \Xi^0\bar{\Xi}^0$	
	BESIII	STCF	BESIII	STCF	BESIII	STCF	BESIII	STCF
α_-	3.8×10^{-3}	2.1×10^{-4}	1.2×10^{-2}	6.5×10^{-4}	2.4×10^{-3}	1.3×10^{-4}	3.2×10^{-3}	1.8×10^{-4}
α_+	3.9×10^{-3}	2.1×10^{-4}	1.2×10^{-2}	6.5×10^{-4}	2.3×10^{-3}	1.3×10^{-4}	3.3×10^{-3}	1.8×10^{-4}
ϕ_Ξ (rad)	—	—	—	—	6.8×10^{-3}	3.7×10^{-4}	9.5×10^{-3}	5.2×10^{-4}
$\bar{\phi}_\Xi$ (rad)	—	—	—	—	6.8×10^{-3}	3.7×10^{-4}	9.5×10^{-3}	5.2×10^{-4}
$ F_A $	1.3×10^{-6}	7.1×10^{-8}	2.1×10^{-6}	1.1×10^{-8}	3.1×10^{-6}	1.7×10^{-7}	4.6×10^{-6}	2.5×10^{-7}
$ d $ (e cm)	8.5×10^{-19}	4.6×10^{-20}	9.7×10^{-19}	5.3×10^{-20}	2.2×10^{-18}	1.2×10^{-19}	3.0×10^{-18}	1.7×10^{-19}
α_-	1.1×10^{-3}	5.9×10^{-5}	1.5×10^{-3}	7.8×10^{-5}	2.0×10^{-3}	1.1×10^{-4}	2.8×10^{-3}	1.5×10^{-4}
α_+	1.1×10^{-3}	5.9×10^{-5}	1.5×10^{-3}	7.8×10^{-5}	2.0×10^{-3}	1.1×10^{-4}	2.8×10^{-3}	1.5×10^{-4}
ϕ_Ξ (rad)	—	—	—	—	4.6×10^{-3}	2.5×10^{-4}	6.3×10^{-3}	3.4×10^{-4}
$\bar{\phi}_\Xi$ (rad)	—	—	—	—	4.6×10^{-3}	2.5×10^{-4}	6.4×10^{-3}	3.5×10^{-4}
$ F_A $	9.8×10^{-7}	5.3×10^{-8}	1.8×10^{-6}	9.7×10^{-8}	2.4×10^{-6}	1.3×10^{-8}	3.5×10^{-6}	1.9×10^{-7}
$ d $ (e cm)	5.5×10^{-19}	3.0×10^{-20}	7.9×10^{-19}	4.3×10^{-20}	1.3×10^{-18}	6.8×10^{-20}	1.1×10^{-18}	6.2×10^{-20}
α_-	2.2×10^{-3}	1.2×10^{-4}	6.9×10^{-3}	3.7×10^{-4}	2.2×10^{-3}	1.2×10^{-4}	3.0×10^{-3}	1.6×10^{-4}
α_+	2.3×10^{-3}	1.2×10^{-4}	6.9×10^{-3}	3.7×10^{-4}	2.2×10^{-3}	1.2×10^{-4}	3.0×10^{-3}	1.6×10^{-4}
ϕ_Ξ (rad)	—	—	—	—	5.8×10^{-3}	3.2×10^{-4}	7.5×10^{-3}	4.1×10^{-4}
$\bar{\phi}_\Xi$ (rad)	—	—	—	—	5.8×10^{-3}	3.2×10^{-4}	7.6×10^{-3}	4.1×10^{-4}
$ F_A $	1.3×10^{-6}	7.0×10^{-8}	1.9×10^{-6}	1.0×10^{-7}	3.1×10^{-6}	1.7×10^{-7}	4.5×10^{-6}	2.5×10^{-7}
$ d $ (e cm)	7.6×10^{-19}	4.1×10^{-20}	8.9×10^{-19}	4.8×10^{-20}	1.8×10^{-18}	9.9×10^{-20}	2.6×10^{-18}	1.4×10^{-19}

TABLE IV: Estimated sensitivities for CP-violating observables A_{CP} and $\Delta\Phi_{CP}$, where the first value is calculated using the corresponding published value of α_- and α_+ .

		$J/\psi \rightarrow \Lambda\bar{\Lambda}$	$J/\psi \rightarrow \Sigma^+\bar{\Sigma}^-$	$J/\psi \rightarrow \Xi^-\bar{\Xi}^+$	$J/\psi \rightarrow \Xi^0\bar{\Xi}^0$
BESIII	A_{CP}	$(-2.7 \pm 4.4) \times 10^{-3}$	$(4.0 \pm 8.5) \times 10^{-3}$	$(6.7 \pm 4.5) \times 10^{-3}$	$(-5.3 \pm 6.1) \times 10^{-3}$
	$\Delta\Phi_{CP}^\Xi$ (rad)	—	—	$(-5.0 \pm 4.9) \times 10^{-3}$	$(-0.1 \pm 6.7) \times 10^{-3}$
STCF	A_{CP}	$(-2.7 \pm 0.1) \times 10^{-3}$	$(4.0 \pm 0.1) \times 10^{-3}$	$(6.7 \pm 0.2) \times 10^{-3}$	$(-5.3 \pm 0.3) \times 10^{-3}$
	$\Delta\Phi_{CP}^\Xi$ (rad)	—	—	$(-5.0 \pm 0.2) \times 10^{-3}$	$(-1.0 \pm 2.8) \times 10^{-4}$

$$\begin{aligned}
& -\frac{E_c^2 \sqrt{E_c^2 - m^2}}{m} H_\sigma F_A^* - 2i E_c^2 \sqrt{E_c^2 - m^2} H_T F_V^* - 2i E_c^2 \sqrt{E_c^2 - m^2} H_T H_\sigma^* - 2i E_c (E_c^2 - m^2) H_T F_A^*, \\
R_{--++} &= 2 \sin^2 \theta (1 - P_T^2 \cos 2\phi) [m^2 |F_V|^2 + \frac{E_c^4}{m^2} |H_\sigma|^2 \\
&\quad - 4E_c^2 (E_c^2 - m^2) |H_T|^2 + 2E_c^2 \operatorname{Re}[F_V H_\sigma^*] - 4i m E_c \sqrt{E_c^2 - m^2} \operatorname{Re}[F_V H_T^*] - \frac{4i E_c^3 \sqrt{E_c^2 - m^2}}{m} \operatorname{Re}[H_\sigma H_T^*]], \\
R_{-+-+} &= (3 + \cos 2\theta + 4P_L \cos \theta + 2P_T^2 \sin^2 \theta \cos 2\phi) \\
&\quad \times [E_c^2 |F_V|^2 + E_c^2 |H_\sigma|^2 + (E_c^2 - m^2) |F_A|^2 \\
&\quad + 2E_c^2 \operatorname{Re}[F_V H_\sigma^*] - 2E_c \sqrt{E_c^2 - m^2} \operatorname{Re}[F_V F_A^*] - 2E_c \sqrt{E_c^2 - m^2} \operatorname{Re}[H_\sigma F_A^*]], \\
R_{-++-} &= [2 \sin^2 \theta + P_T^2 (3 \cos 2\phi + \cos 2\theta \cos 2\phi - 4i \cos \theta \sin 2\phi)] \\
&\quad \times [E_c^2 |F_V|^2 + E_c^2 |H_\sigma|^2 - (E_c^2 - m^2) |F_A|^2 \\
&\quad + 2E_c^2 \operatorname{Re}[F_V H_\sigma^*] + 2i E_c \sqrt{E_c^2 - m^2} \operatorname{Im}[F_V F_A^*] + 2i E_c \sqrt{E_c^2 - m^2} \operatorname{Im}[H_\sigma F_A^*]], \\
R_{+-+-} &= [2 \sin^2 \theta + P_T^2 (3 \cos 2\phi + \cos 2\theta \cos 2\phi + 4i \cos \theta \sin 2\phi)] \\
&\quad \times [E_c^2 |F_V|^2 + E_c^2 |H_\sigma|^2 - (E_c^2 - m^2) |F_A|^2 \\
&\quad + 2E_c^2 \operatorname{Re}[F_V H_\sigma^*] - 2i \operatorname{Im}[F_V F_A^*] E_c \sqrt{E_c^2 - m^2} - 2i E_c \sqrt{E_c^2 - m^2} \operatorname{Im}[H_\sigma F_A^*]], \\
R_{+-+-} &= [3 + \cos 2\theta - 4P_L \cos \theta + 2P_T^2 \sin^2 \theta \cos 2\phi] \\
&\quad \times [E_c^2 |F_V|^2 + E_c^2 |H_\sigma|^2 + (E_c^2 - m^2) |F_A|^2 \\
&\quad + 2E_c^2 \operatorname{Re}[F_V H_\sigma^*] + 2E_c \sqrt{E_c^2 - m^2} \operatorname{Re}[F_V F_A^*] + 2E_c \sqrt{E_c^2 - m^2} \operatorname{Re}[H_\sigma F_A^*]], \\
R_{++--} &= 2 \sin^2 \theta (1 - P_T^2 \cos 2\phi) \\
&\quad \times [m^2 |F_V|^2 + \frac{E_c^4}{m^2} |H_\sigma|^2 - 4E_c^2 (E_c^2 - m^2) |H_T|^2 \\
&\quad + \frac{4i E_c^3 \sqrt{E_c^2 - m^2}}{m} \operatorname{Re}[H_\sigma H_T^*] + 2E_c^2 \operatorname{Re}[F_V H_\sigma^*] + 4i m E_c \sqrt{E_c^2 - m^2} \operatorname{Re}[F_V H_T^*]], \\
R_{--+-} &= 2 \sin \theta [\cos \theta + P_L - P_T^2 (\cos \theta \cos 2\phi + i \sin 2\phi)] \\
&\quad \times [m E_c |F_V|^2 + \frac{E_c^3}{m} |H_\sigma|^2 + \frac{E_c^3}{m} H_\sigma F_V^* + m E_c F_V H_\sigma^* - m \sqrt{E_c^2 - m^2} F_V F_A^* \\
&\quad - \frac{E_c^2 \sqrt{E_c^2 - m^2}}{m} H_\sigma F_A^* - 2i E_c^2 \sqrt{E_c^2 - m^2} H_T F_V^* - 2i E_c^2 \sqrt{E_c^2 - m^2} H_T H_\sigma^* + 2i E_c (E_c^2 - m^2) H_T F_A^*], \\
R_{--+-} &= 2 \sin \theta [\cos \theta - P_L - P_T^2 (\cos \theta \cos 2\phi - i \sin 2\phi)] \\
&\quad \times [-m E_c |F_V|^2 - \frac{E_c^3}{m} |H_\sigma|^2 - \frac{E_c^3}{m} H_\sigma F_V^* - m E_c F_V H_\sigma^* - m \sqrt{E_c^2 - m^2} F_V F_A^* \\
&\quad - \frac{E_c^2 \sqrt{E_c^2 - m^2}}{m} H_\sigma F_A^* + 2i E_c^2 \sqrt{E_c^2 - m^2} H_T F_V^* + 2i E_c^2 \sqrt{E_c^2 - m^2} H_T H_\sigma^* + 2i E_c (E_c^2 - m^2) H_T F_A^*], \\
R_{-+--} &= 2 \sin \theta [\cos \theta + P_L - P_T^2 (\cos \theta \cos 2\phi - i \sin 2\phi)] \\
&\quad \times [m E_c |F_V|^2 + \frac{E_c^3}{m} |H_\sigma|^2 + \frac{E_c^3}{m} H_\sigma^* F_V + m E_c F_V^* H_\sigma - m \sqrt{E_c^2 - m^2} F_A F_V^* \\
&\quad - \frac{E_c^2 \sqrt{E_c^2 - m^2}}{m} F_A H_\sigma^* + 2i E_c^2 \sqrt{E_c^2 - m^2} F_V H_T^* + 2i E_c^2 \sqrt{E_c^2 - m^2} H_\sigma H_T^* - 2i E_c (E_c^2 - m^2) F_A H_T^*], \\
R_{+---} &= 2 \sin \theta [\cos \theta - P_L - P_T^2 (\cos \theta \cos 2\phi + i \sin 2\phi)] \\
&\quad \times [-m E_c |F_V|^2 - \frac{E_c^3}{m} |H_\sigma|^2 - \frac{E_c^3}{m} F_V H_\sigma^* - m E_c H_\sigma F_V^* - m \sqrt{E_c^2 - m^2} F_A F_V^* \\
&\quad - \frac{E_c^2 \sqrt{E_c^2 - m^2}}{m} F_A H_\sigma^* - 2i E_c^2 \sqrt{E_c^2 - m^2} F_V H_T^* - 2i E_c^2 \sqrt{E_c^2 - m^2} H_\sigma H_T^* - 2i E_c (E_c^2 - m^2) F_A H_T^*], \\
R_{----} &= 2 \sin^2 \theta [1 - P_T^2 \cos 2\phi] \\
&\quad \times [m^2 |F_V|^2 + \frac{E_c^4}{m^2} |H_\sigma|^2 + 4E_c^2 (E_c^2 - m^2) |H_T|^2
\end{aligned}$$

$$+2E_c^2\text{Re}[F_VH_\sigma^*]-4mE_c\sqrt{E_c^2-m^2}\text{Im}[F_VH_T^*]-\frac{4E_c^3\sqrt{E_c^2-m^2}}{m}\text{Im}[H_\sigma H_T^*]. \quad (\text{A1})$$

Here, the symbols $+(-)$ represent the helicity $\lambda_1(\lambda_2)$ as $+1/2(-1/2)$, while m denotes the mass of B hyperon which decays via J/ψ .

Appendix B: Decay SDM of hyperons

The decay SDM T for a hyperon decay can be expressed as:

$$\begin{aligned} T_{++++} &= \frac{1}{4}(1+\alpha_D)(1+\cos\theta), \\ T_{-+++} &= \frac{1}{4}(1+\alpha_D)\sin\theta(\cos\phi-i\sin\phi), \\ T_{+-++} &= \frac{1}{4}(i\beta_D-\gamma_D)\sin\theta, \\ T_{+++-} &= \frac{1}{4}(1+\alpha_D)\sin\theta(\cos\phi+i\sin\phi), \\ T_{+++-} &= -\frac{1}{4}(i\beta_D+\gamma_D)\sin\theta, \\ T_{--++} &= -\frac{1}{4}(i\beta_D-\gamma_D)(1+\cos\theta)(\cos\phi-i\sin\phi), \\ T_{-+-+} &= \frac{1}{4}(1+\alpha_D)(1-\cos\theta), \\ T_{-+-+} &= -\frac{1}{4}(i\beta_D+\gamma_D)(1-\cos\theta)(\cos\phi-i\sin\phi), \\ T_{+-+-} &= \frac{1}{4}(i\beta_D-\gamma_D)(1-\cos\theta)(\cos\phi+i\sin\phi), \end{aligned}$$

$$\begin{aligned} T_{+-+-} &= \frac{1}{4}(1-\alpha_D)(1-\cos\theta), \\ T_{+---} &= \frac{1}{4}(i\beta_D+\gamma_D)(1+\cos\theta)(\cos\phi+i\sin\phi), \\ T_{---+} &= -\frac{1}{4}(i\beta_D-\gamma_D)\sin\theta, \\ T_{--+-} &= -\frac{1}{4}(1-\alpha_D)\sin\theta(\cos\phi-i\sin\phi), \\ T_{-+--} &= \frac{1}{4}(i\beta_D+\gamma_D)\sin\theta, \\ T_{+---} &= -\frac{1}{4}(1-\alpha_D)\sin\theta(\cos\phi+i\sin\phi), \\ T_{----} &= \frac{1}{4}(1-\alpha_D)(1+\cos\theta). \end{aligned} \quad (\text{B1})$$

For instance, in the decay process $\Xi^- \rightarrow \Lambda\pi^-$, where θ and ϕ denote the polar and azimuthal angles of the decay, the parameters α_D , β_D , and γ_D , as defined in Ref. [94], are replaced with those specific to Ξ . For the subsequent decay $\Lambda \rightarrow p\pi^-$, the helicity angles and parameters are replaced with those for Λ . Then, the complete decay SDM for the two-step decay of Ξ^- is obtained by the product of the decay SDMs for Ξ^- and Λ . By utilizing these parameters, we can establish the joint angular distribution form for any decay process.

Appendix C: Isospin decomposition

In this section, we present the correspondence between CP violation observables and the weak and strong phase angles in the decay processes of Λ , Σ^+ , Ξ^- and Ξ^0 hyperons.

The decay amplitudes for $\Lambda \rightarrow p\pi^-$ are [51]

$$A_S = -\frac{\sqrt{2}}{\sqrt{3}}S_{11}e^{i(\delta_1^S + \phi_{11}^S)} + \frac{1}{\sqrt{3}}S_{33}e^{i(\delta_3^S + \phi_{33}^S)}, \quad (\text{C1})$$

$$A_P = -\frac{\sqrt{2}}{\sqrt{3}}P_{11}e^{i(\delta_1^P + \phi_{11}^P)} + \frac{1}{\sqrt{3}}P_{33}e^{i(\delta_3^P + \phi_{33}^P)}. \quad (\text{C2})$$

Experimentally we know that $\Delta I = 3/2$ amplitudes are smaller than $\Delta I = 1/2$ amplitudes. If we work to first order in the $\Delta I = 3/2$ amplitude and the weak-interaction phases, we find

$$\begin{aligned} A_{CP} &= -\tan(\delta_1^P - \delta_1^S)\tan(\phi_{11}^P - \phi_{11}^S) \left[1 - \frac{1}{\sqrt{2}}\frac{S_{33}}{S_{11}} \left(\frac{\sin(\delta_1^P - \delta_3^S)\sin(\phi_{11}^P - \phi_{33}^S)}{\sin(\delta_1^P - \delta_1^S)\sin(\phi_{11}^P - \phi_{11}^S)} - 1 \right) \right. \\ &\quad \left. - \frac{1}{\sqrt{2}}\frac{P_{33}}{P_{11}} \left(\frac{\sin(\delta_3^P - \delta_1^S)\sin(\phi_{33}^P - \phi_{11}^S)}{\sin(\delta_1^P - \delta_1^S)\sin(\phi_{11}^P - \phi_{11}^S)} - 1 \right) + \frac{1}{2}\frac{S_{33}P_{33}}{S_{11}P_{11}} \left(\frac{\sin(\delta_3^P - \delta_3^S)\sin(\phi_{33}^P - \phi_{33}^S)}{\sin(\delta_1^P - \delta_1^S)\sin(\phi_{11}^P - \phi_{11}^S)} - 1 \right) \right], \end{aligned} \quad (\text{C3})$$

$$B_{CP} = \tan(\phi_{11}^P - \phi_{11}^S) \left[1 - \frac{1}{\sqrt{2}}\frac{S_{33}}{S_{11}} \left(\frac{\sin(\phi_{11}^P - \phi_{33}^S)}{\sin(\phi_{11}^P - \phi_{11}^S)} - 1 \right) \right]$$

$$-\frac{1}{\sqrt{2}} \frac{P_{33}}{P_{11}} \left(\frac{\sin(\phi_{33}^P - \phi_{11}^S)}{\sin(\phi_{11}^P - \phi_{11}^S)} - 1 \right) + \frac{1}{2} \frac{S_{33} P_{33}}{S_{11} P_{11}} \left(\frac{\sin(\phi_{33}^P - \phi_{33}^S)}{\sin(\phi_{11}^P - \phi_{11}^S)} - 1 \right) \Bigg], \quad (\text{C4})$$

$$\Delta C = \tan(\delta_1^P - \delta_1^S) \left[1 - \frac{1}{\sqrt{2}} \frac{S_{33}}{S_{11}} \left(\frac{\sin(\delta_1^P - \delta_3^S)}{\sin(\delta_1^P - \delta_1^S)} - 1 \right) \right. \\ \left. - \frac{1}{\sqrt{2}} \frac{P_{33}}{P_{11}} \left(\frac{\sin(\delta_3^P - \delta_1^S)}{\sin(\delta_1^P - \delta_1^S)} - 1 \right) + \frac{1}{2} \frac{S_{33} P_{33}}{S_{11} P_{11}} \left(\frac{\sin(\delta_3^P - \delta_3^S)}{\sin(\delta_1^P - \delta_1^S)} - 1 \right) \right]. \quad (\text{C5})$$

The decay amplitudes for $\Sigma^+ \rightarrow p\pi^0$ are [51]

$$A_S = -\frac{\sqrt{2}}{3} \left(S_{11} e^{i\phi_{11}^S} + \frac{1}{2} S_{31} e^{i\phi_{31}^S} \right) e^{i\delta_1^S} + \frac{\sqrt{2}}{3} \left(S_{13} e^{i\phi_{13}^S} - \frac{2\sqrt{2}}{\sqrt{5}} S_{33} e^{i\phi_{33}^S} \right) e^{i\delta_3^S}, \quad (\text{C6})$$

$$A_P = -\frac{\sqrt{2}}{3} \left(P_{11} e^{i\phi_{11}^P} + \frac{1}{2} S_{31} e^{i\phi_{31}^P} \right) e^{i\delta_1^P} + \frac{\sqrt{2}}{3} \left(P_{13} e^{i\phi_{13}^P} - \frac{2\sqrt{2}}{\sqrt{5}} P_{33} e^{i\phi_{33}^P} \right) e^{i\delta_3^P}. \quad (\text{C7})$$

Calculating the decay asymmetries we obtain

$$A_{CP} = -\tan(\delta_1^P - \delta_1^S) \tan(\bar{\phi}_1^P - \bar{\phi}_1^S) \left[1 - \frac{\bar{S}_3}{\bar{S}_1} \left(\frac{\sin(\delta_1^P - \delta_3^S) \sin(\bar{\phi}_1^P - \bar{\phi}_3^S)}{\sin(\delta_1^P - \delta_1^S) \sin(\bar{\phi}_1^P - \bar{\phi}_1^S)} - 1 \right) \right. \\ \left. - \frac{\bar{P}_3}{\bar{P}_1} \left(\frac{\sin(\delta_3^P - \delta_3^S) \sin(\bar{\phi}_3^P - \bar{\phi}_3^S)}{\sin(\delta_1^P - \delta_1^S) \sin(\bar{\phi}_1^P - \bar{\phi}_1^S)} - 1 \right) + \frac{\bar{S}_3 \bar{P}_3}{\bar{S}_1 \bar{P}_1} \left(\frac{\sin(\delta_3^P - \delta_3^S) \sin(\bar{\phi}_3^P - \bar{\phi}_3^S)}{\sin(\delta_1^P - \delta_1^S) \sin(\bar{\phi}_1^P - \bar{\phi}_1^S)} - 1 \right) \right], \quad (\text{C8})$$

$$B_{CP} = \tan(\bar{\phi}_1^P - \bar{\phi}_1^S) \times \left[1 - \frac{\bar{S}_3}{\bar{S}_1} \left(\frac{\sin(\bar{\phi}_1^P - \bar{\phi}_3^S)}{\sin(\bar{\phi}_1^P - \bar{\phi}_1^S)} - 1 \right) - \frac{\bar{P}_3}{\bar{P}_1} \left(\frac{\sin(\bar{\phi}_3^P - \bar{\phi}_1^S)}{\sin(\bar{\phi}_1^P - \bar{\phi}_1^S)} - 1 \right) + \frac{\bar{S}_3 \bar{P}_3}{\bar{S}_1 \bar{P}_1} \left(\frac{\sin(\bar{\phi}_3^P - \bar{\phi}_3^S)}{\sin(\bar{\phi}_1^P - \bar{\phi}_1^S)} - 1 \right) \right], \quad (\text{C9})$$

$$\Delta C = \tan(\delta_1^P - \delta_1^S) \times \left[1 - \frac{\bar{S}_3}{\bar{S}_1} \left(\frac{\sin(\delta_1^P - \delta_3^S)}{\sin(\delta_1^P - \delta_1^S)} - 1 \right) - \frac{\bar{P}_3}{\bar{P}_1} \left(\frac{\sin(\delta_3^P - \delta_1^S)}{\sin(\delta_1^P - \delta_1^S)} - 1 \right) + \frac{\bar{S}_3 \bar{P}_3}{\bar{S}_1 \bar{P}_1} \left(\frac{\sin(\delta_3^P - \delta_3^S)}{\sin(\delta_1^P - \delta_1^S)} - 1 \right) \right], \quad (\text{C10})$$

where

$$\bar{S}_1 = S_{11} + \frac{1}{2} S_{31}, \quad \bar{S}_3 = S_{13} - 2\sqrt{\frac{2}{5}} S_{33}, \quad (\text{C11})$$

$$\bar{\phi}_1^S = \frac{S_{11} \phi_{11}^S + \frac{1}{2} S_{31} \phi_{31}^S}{S_{11} + \frac{1}{2} S_{31}}, \quad \bar{\phi}_3^S = \frac{S_{13} \phi_{13}^S - 2\sqrt{\frac{2}{5}} S_{33} \phi_{33}^S}{S_{13} - 2\sqrt{\frac{2}{5}} S_{33}}. \quad (\text{C12})$$

The decay amplitudes for $\Xi^- \rightarrow \Lambda\pi^-$ are [51]

$$A_S = \left(S_{12} e^{i\phi_{12}^S} + \frac{1}{2} S_{32} e^{i\phi_{32}^S} \right) e^{i\delta_2^S}, \quad (\text{C13})$$

$$A_P = \left(P_{12} e^{i\phi_{12}^P} + \frac{1}{2} P_{32} e^{i\phi_{32}^P} \right) e^{i\delta_2^P}. \quad (\text{C14})$$

The discussion goes completely parallel to that for Λ decay and we find

$$A_{CP} = -\tan(\delta_2^P - \delta_2^S) \tan(\phi_{12}^P - \phi_{12}^S) \left[1 + \frac{1}{2} \frac{S_{32}}{S_{12}} \left(\frac{\sin(\phi_{12}^P - \phi_{32}^S)}{\sin(\phi_{12}^P - \phi_{12}^S)} - 1 \right) \right. \\ \left. + \frac{1}{2} \frac{P_{32}}{P_{12}} \left(\frac{\sin(\phi_{32}^P - \phi_{12}^S)}{\sin(\phi_{12}^P - \phi_{12}^S)} - 1 \right) + \frac{1}{4} \frac{S_{32} P_{32}}{S_{12} P_{12}} \left(\frac{\sin(\phi_{32}^P - \phi_{32}^S)}{\sin(\phi_{12}^P - \phi_{12}^S)} - 1 \right) \right], \quad (\text{C15})$$

$$B_{CP} = \tan(\phi_{12}^P - \phi_{12}^S) \left[1 + \frac{1}{2} \frac{S_{32}}{S_{12}} \left(\frac{\sin(\phi_{12}^P - \phi_{32}^S)}{\sin(\phi_{12}^P - \phi_{12}^S)} - 1 \right) + \frac{1}{2} \frac{P_{32}}{P_{12}} \left(\frac{\sin(\phi_{32}^P - \phi_{12}^S)}{\sin(\phi_{12}^P - \phi_{12}^S)} - 1 \right) + \frac{1}{4} \frac{S_{32}P_{32}}{S_{12}P_{12}} \left(\frac{\sin(\phi_{32}^P - \phi_{32}^S)}{\sin(\phi_{12}^P - \phi_{12}^S)} - 1 \right) \right], \quad (\text{C16})$$

$$\Delta C = \tan(\delta_2^P - \delta_2^S). \quad (\text{C17})$$

while for $\Xi^0 \rightarrow \Lambda\pi^0$

$$A_S = \frac{1}{\sqrt{2}} (S_{12} e^{i\phi_{12}^S} - S_{32} e^{i\phi_{32}^S}) e^{i\delta_2^S}, \quad (\text{C18})$$

$$A_P = \frac{1}{\sqrt{2}} (P_{12} e^{i\phi_{12}^P} - P_{32} e^{i\phi_{32}^P}) e^{i\delta_2^P}. \quad (\text{C19})$$

And we have

$$A_{CP} = -\tan(\delta_2^P - \delta_2^S) \tan(\phi_{12}^P - \phi_{12}^S) \times \left[1 - \frac{S_{32}}{S_{12}} \left(\frac{\sin(\phi_{12}^P - \phi_{32}^S)}{\sin(\phi_{12}^P - \phi_{12}^S)} - 1 \right) - \frac{P_{32}}{P_{12}} \left(\frac{\sin(\phi_{32}^P - \phi_{12}^S)}{\sin(\phi_{12}^P - \phi_{12}^S)} - 1 \right) + \frac{S_{32}P_{32}}{S_{12}P_{12}} \left(\frac{\sin(\phi_{32}^P - \phi_{32}^S)}{\sin(\phi_{12}^P - \phi_{12}^S)} - 1 \right) \right], \quad (\text{C20})$$

$$B_{CP} = \tan(\phi_{12}^P - \phi_{12}^S) \times \left[1 - \frac{S_{32}}{S_{12}} \left(\frac{\sin(\phi_{12}^P - \phi_{32}^S)}{\sin(\phi_{12}^P - \phi_{12}^S)} - 1 \right) - \frac{P_{32}}{P_{12}} \left(\frac{\sin(\phi_{32}^P - \phi_{12}^S)}{\sin(\phi_{12}^P - \phi_{12}^S)} - 1 \right) + \frac{S_{32}P_{32}}{S_{12}P_{12}} \left(\frac{\sin(\phi_{32}^P - \phi_{32}^S)}{\sin(\phi_{12}^P - \phi_{12}^S)} - 1 \right) \right], \quad (\text{C21})$$

$$\Delta C = \tan(\delta_2^P - \delta_2^S). \quad (\text{C22})$$

Appendix D: Sensitivity curve

The sensitivities to the weak decay parameters α_- and α_+ (including the ϕ_Ξ and $\bar{\phi}_\Xi$ for Ξ^- and Ξ^0 hy-

peron decay), the P-violating term F_A , and the EDM for Λ , Σ^+ , Ξ^- and Ξ^0 hyperon are depicted in Figs. 5, 6, 7 and 8. The range of events covers the statistics that can be collected by BESIII, and the subgraph shows the sensitivity distribution around the STCF statistics.

-
- [1] G. Gamow, *Phys. Rev.* **70**, 572 (1946).
- [2] G. Gamow, *Phys. Rev.* **71**, 273 (1947).
- [3] A. Julie *et al.*, Louis Savenien Dupuis Journal of Multi-disciplinary Research **10.21839/lsdjm.r.2023.v2.23** (2023).
- [4] A. D. Sakharov, *Pisma Zh. Eksp. Teor. Fiz.* **5**, 32 (1967).
- [5] J. H. Christenson, J. W. Cronin, V. L. Fitch, and R. Turlay, *Phys. Rev. Lett.* **13**, 138 (1964).
- [6] B. Aubert *et al.* (BABAR Collaboration), *Phys. Rev. Lett.* **87**, 091801 (2001).
- [7] K. Abe *et al.* (Belle Collaboration), *Phys. Rev. Lett.* **87**, 091802 (2001).
- [8] R. Aaij *et al.* (LHCb Collaboration), *Phys. Rev. Lett.* **122**, 211803 (2019).
- [9] N. Cabibbo, *Phys. Rev. Lett.* **10**, 531 (1963).
- [10] M. Kobayashi and T. Maskawa, *Prog. Theor. Phys.* **49**, 652 (1973), <https://academic.oup.com/ptp/article-pdf/49/2/652/5257692/49-2-652.pdf>.
- [11] R. Jackiw and C. Rebbi, *Phys. Rev. Lett.* **37**, 172 (1976).
- [12] V. Baluni, *Phys. Rev. D* **19**, 2227 (1979).
- [13] B. K. Sahoo, *Phys. Rev. D* **95**, 013002 (2017).
- [14] S. Weinberg, *Phys. Rev. D* **11**, 3583 (1975).
- [15] R. D. Peccei, in *Axions: Theory, Cosmology, and Experimental Searches*, edited by M. Kuster, G. Raffelt, and B. Beltrán (Springer Berlin Heidelberg, Berlin, Heidelberg, 2008) pp. 3–17.
- [16] J. E. Kim and G. Carosi, *Rev. Mod. Phys.* **82**, 557 (2010).
- [17] E. M. Purcell and N. F. Ramsey, *Phys. Rev.* **78**, 807 (1950).
- [18] L. Landau, *Nuclear Physics* **3**, 127 (1957).
- [19] W. Bernreuther and M. Suzuki, *Reviews of Modern Physics* **63**, 313 (1991).
- [20] J. Schwinger, *Phys. Rev.* **82**, 914 (1951).
- [21] G. Lüders, *Annals of Physics* **2**, 1 (1957).
- [22] M. C. Weisskopf *et al.*, *Phys. Rev. Lett.* **21**, 1645 (1968).
- [23] K. Abdullah *et al.*, *Phys. Rev. Lett.* **65**, 2347 (1990).
- [24] J. Baron *et al.* (ACME Collaboration), *Science* **343**, 269 (2014).
- [25] V. Andreev *et al.* (ACME Collaboration), *Nature (London)* **562**, 355 (2018).
- [26] T. S. Roussy *et al.*, *Science* **381**, 46 (2023), <https://www.science.org/doi/pdf/10.1126/science.adg4084>.
- [27] J. Bailey *et al.* (CERN Muon Storage Ring), *J. Phys. G* **4**, 345 (1978).

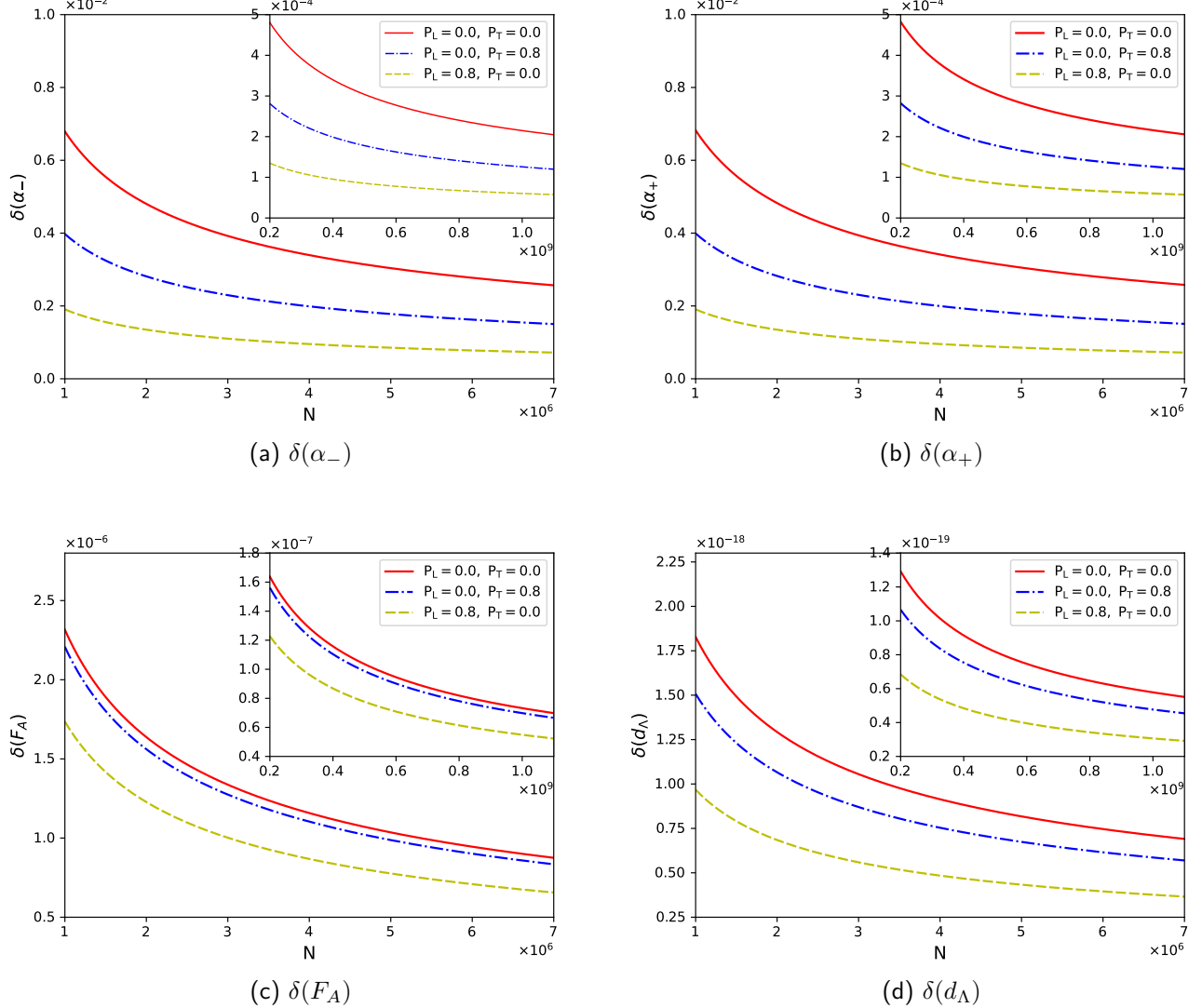


FIG. 5: Sensitivities for decay parameters (a) α_- and (b) α_+ , (c) P-violating term F_A , and (d) electric dipole moment d_Λ in $J/\psi \rightarrow \Lambda(\rightarrow p\pi^-)\bar{\Lambda}(\rightarrow \bar{p}\pi^+)$ decays.

- [28] G. W. Bennett *et al.* (Muon (g-2) Collaboration), *Phys. Rev. D* **80**, 052008 (2009).
- [29] F. del Aguila and M. Sher, *Phys. Lett. B* **252**, 116 (1990).
- [30] H. Albrecht *et al.* (ARGUS Collaboration), *Phys. Lett. B* **485**, 37 (2000).
- [31] K. Inami *et al.* (Belle Collaboration), *Phys. Lett. B* **551**, 16 (2003).
- [32] Y. Ema, T. Gao, and M. Pospelov, *Phys. Lett. B* **835**, 137496 (2022), arXiv:2207.01679 [hep-ph].
- [33] J. H. Smith, E. M. Purcell, and N. F. Ramsey, *Phys. Rev.* **108**, 120 (1957).
- [34] I. S. Altarev *et al.*, *JETP Lett. (USSR)* (Engl. Transl.); (*United States*) **29**:12 (1979).
- [35] J. M. Pendlebury *et al.*, *Phys. Rev. D* **92**, 092003 (2015).
- [36] C. Abel *et al.*, *Phys. Rev. Lett.* **124**, 081803 (2020).
- [37] J. P. Jacobs *et al.*, *Phys. Rev. A* **52**, 3521 (1995).
- [38] M. V. Romalis *et al.*, *Phys. Rev. Lett.* **86**, 2505 (2001).
- [39] W. C. Griffith *et al.*, *Phys. Rev. Lett.* **102**, 101601 (2009).
- [40] B. Graner, Y. Chen, E. G. Lindahl, and B. R. Heckel, *Phys. Rev. Lett.* **116**, 161601 (2016).
- [41] G. E. Harrison, P. G. H. Sandars, and S. J. Wright, *Phys. Rev. Lett.* **22**, 1263 (1969).
- [42] V. F. Dmitriev and R. A. Sen'kov, *Phys. Rev. Lett.* **91**, 212303 (2003).
- [43] B. K. Sahoo, *Phys. Rev. D* **95**, 013002 (2017).
- [44] L. Pondrom *et al.*, *Phys. Rev. D* **23**, 814 (1981).
- [45] A. Pich and E. de Rafael, *Nuclear Physics* **367**, 313 (1991).
- [46] D. Atwood and A. Soni, *Physics Letters B* **291**, 293 (1992).
- [47] B. Borasoy, *Phys. Rev. D* **61**, 114017 (2000).
- [48] F.-K. Guo and U.-G. Meissner, *Journal of High Energy Physics* **2012** (2012).
- [49] T. D. Lee and C. N. Yang, *Phys. Rev.* **108**, 1645 (1957).
- [50] J. F. Donoghue and S. Pakvasa, *Phys. Rev. Lett.* **55**, 162 (1985).
- [51] J. F. Donoghue, X.-G. He, and S. Pakvasa, *Phys. Rev. D* **34**, 833 (1986).
- [52] J. Tandean and G. Valencia, *Phys. Rev. D* **67**, 056001 (2003).
- [53] J. T. DONOHUE, *Phys. Rev.* **178**, 2288 (1969).
- [54] H. Chen and R.-G. Ping, *Phys. Rev. D* **76**, 036005 (2007).
- [55] E. Perotti, G. Fäldt, A. Kupsc, S. Leupold, and J. J. Song, *Phys. Rev. D* **99**, 056008 (2019), arXiv:1809.04038 [hep-ph].
- [56] Z. Zhang, J. J. Song, and Y.-j. Zhou, *Phys. Rev. D* **109**, 036005 (2024), arXiv:2312.04363 [hep-ph].
- [57] A. Z. Dubničká *et al.*, *Il Nuovo Cimento A* (1965-1970) **109**, 10.1007/BF02731012 (1996).
- [58] E. Tomasi-Gustafsson, F. Lacroix, C. Duterte, and G. I. Gakh, *Eur. Phys. J. A* **24**, 419 (2005), arXiv:nucl-th/0503001.
- [59] H. Czyz *et al.*, *Phys. Rev. D* **75**, 074026 (2007).
- [60] G. Fäldt and A. Kupsc, *Phys. Lett. B* **772**, 16 (2017), arXiv:1702.07288 [hep-ph].
- [61] N. Salone, P. Adlarson, V. Batozskaya, A. Kupsc, S. Leupold, and J. Tandean, *Phys. Rev. D* **105**, 116022 (2022), arXiv:2203.03035 [hep-ph].
- [62] Z. Zhang, J.-p. Lv, Z.-h. Yu, and Z.-t. Liang, *Phys. Rev. D* **110**, 074019 (2024), arXiv:2406.03840 [hep-ph].
- [63] V. Batozskaya, A. Kupsc, N. Salone, and J. Wiechnik, *Phys. Rev. D* **108**, 016011 (2023), arXiv:2302.07665 [hep-ph].
- [64] M. Ablikim *et al.*, *Nuclear Instruments and Methods in Physics Research Section A: Accelerators, Spectrometers, Detectors and Associated Equipment* **614**, 345 (2010).
- [65] M. Ablikim *et al.*, *Chinese Physics C* **44**, 040001 (2020).
- [66] M. Ablikim *et al.* (BESIII Collaboration), *Chinese Physics C* **46**, 074001 (2022).
- [67] M. Ablikim *et al.* (BESIII Collaboration), *Phys. Rev. Lett.* **129**, 131801 (2022).
- [68] M. Ablikim *et al.* (BESIII Collaboration), *J. High Energ. Phys.* **2023**.
- [69] M. Ablikim *et al.* (BESIII Collaboration), *Phys. Rev. D* **105**, L011101 (2022).
- [70] M. Ablikim *et al.* (BESIII Collaboration), *Phys. Rev. Lett.* **125**, 052004 (2020).
- [71] M. Ablikim *et al.* (BESIII Collaboration), *Phys. Rev. D* **106**, L091101 (2022).
- [72] M. Ablikim *et al.* (BESIII Collaboration), *Nature* **606**, 64–69 (2022).
- [73] M. Ablikim *et al.* (BESIII Collaboration), *Phys. Rev. D* **108**, L031106 (2023).
- [74] M. Ablikim *et al.* (BESIII Collaboration), *Phys. Rev. D* **108**, L011101 (2023).
- [75] M. Ablikim *et al.* (BESIII Collaboration), *Phys. Rev. D* **100**, 051101 (2019).
- [76] *Phys. Rev. Lett.* **126**, 092002 (2021).
- [77] X. G. He and J. P. Ma, *Phys. Lett. B* **839**, 137834 (2023), arXiv:2212.08243 [hep-ph].
- [78] Y. Du, X.-G. He, J.-P. Ma, and X.-Y. Du, *Phys. Rev. D* **110**, 076019 (2024).
- [79] Z. Zhang, R.-G. Ping, T. Liu, J. J. Song, W. Yang, and Y.-j. Zhou, *Phys. Rev. D* **110**, 034034 (2024).
- [80] N. Salone, P. Adlarson, V. Batozskaya, A. Kupsc, S. Leupold, and J. Tandean, *Phys. Rev. D* **105**, 116022 (2022).
- [81] S. Zeng, Y. Xu, X. R. Zhou, J. J. Qin, and B. Zheng, *Chin. Phys. C* **47**, 113001 (2023), arXiv:2306.15602 [hep-ex].
- [82] Z. Zhang and J.-J. Song, *Chinese Physics C* **47**, 093101 (2023).
- [83] X. Cao, Y.-T. Liang, and R.-G. Ping, *Phys. Rev. D* **110**, 014035 (2024).
- [84] J. Fu, H.-B. Li, J.-P. Wang, F.-S. Yu, and J. Zhang, *Phys. Rev. D* **108**, L091301 (2023), arXiv:2307.04364 [hep-ex].
- [85] M. Achasov *et al.*, *Front. Phys. (Beijing)* **19**, 14701 (2024), arXiv:2303.15790 [hep-ex].
- [86] A. A. Sokolov and I. M. Ternov, *Dokl. Akad. Nauk SSSR* **153**, 1052 (1963).
- [87] X.-G. He, J. P. Ma, and B. McKellar, *Phys. Rev. D* **47**, R1744 (1993).
- [88] M. N. Rosenbluth, *Phys. Rev.* **79**, 615 (1950).
- [89] J. G. Korner and M. Kuroda, *Phys. Rev. D* **16**, 2165 (1977).
- [90] X.-G. He, J. P. Ma, and B. McKellar, *Phys. Rev. D* **49**, 4548 (1994).
- [91] M. Ablikim *et al.* (BESIII Collaboration), *Phys. Rev. Lett.* **132**, 101801 (2024).
- [92] O. Behnke *et al.*, (Wiley-VCH, Weinheim, Germany, 2013).
- [93] R. L. Workman *et al.* (Particle Data Group), *PTEP* **2022**, 083C01 (2022).
- [94] M. Tanabashi *et al.* (Particle Data Group), *Phys. Rev. D* **98**, 030001 (2018).

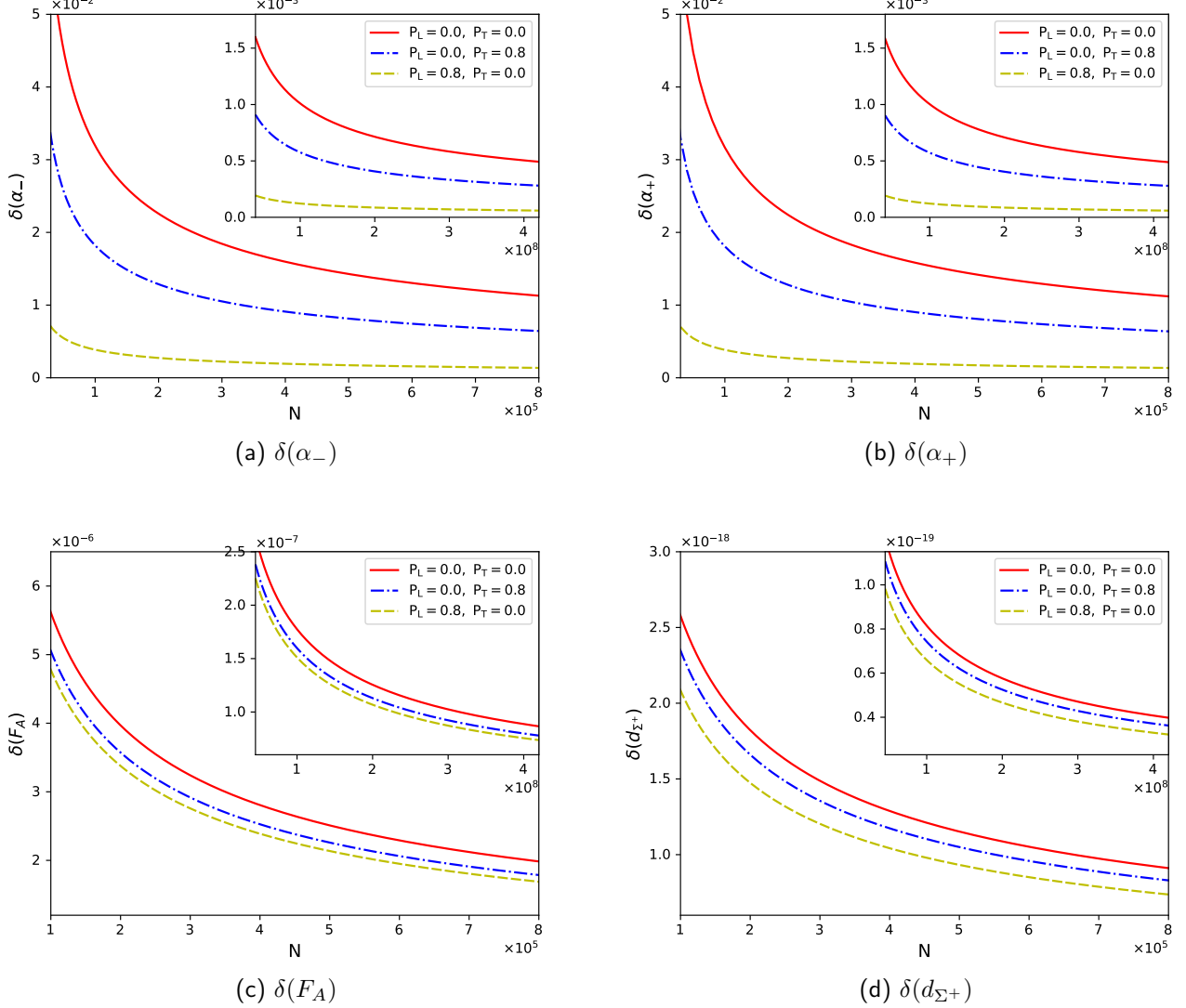


FIG. 6: Sensitivities for decay parameters (a) α_- and (b) α_+ , (c) P-violating term F_A , and (d) electric dipole moment d_{Σ^+} in $J/\psi \rightarrow \Sigma^+ (\rightarrow p\pi^0) \bar{\Sigma}^- (\rightarrow \bar{p}\pi^0)$ decays.

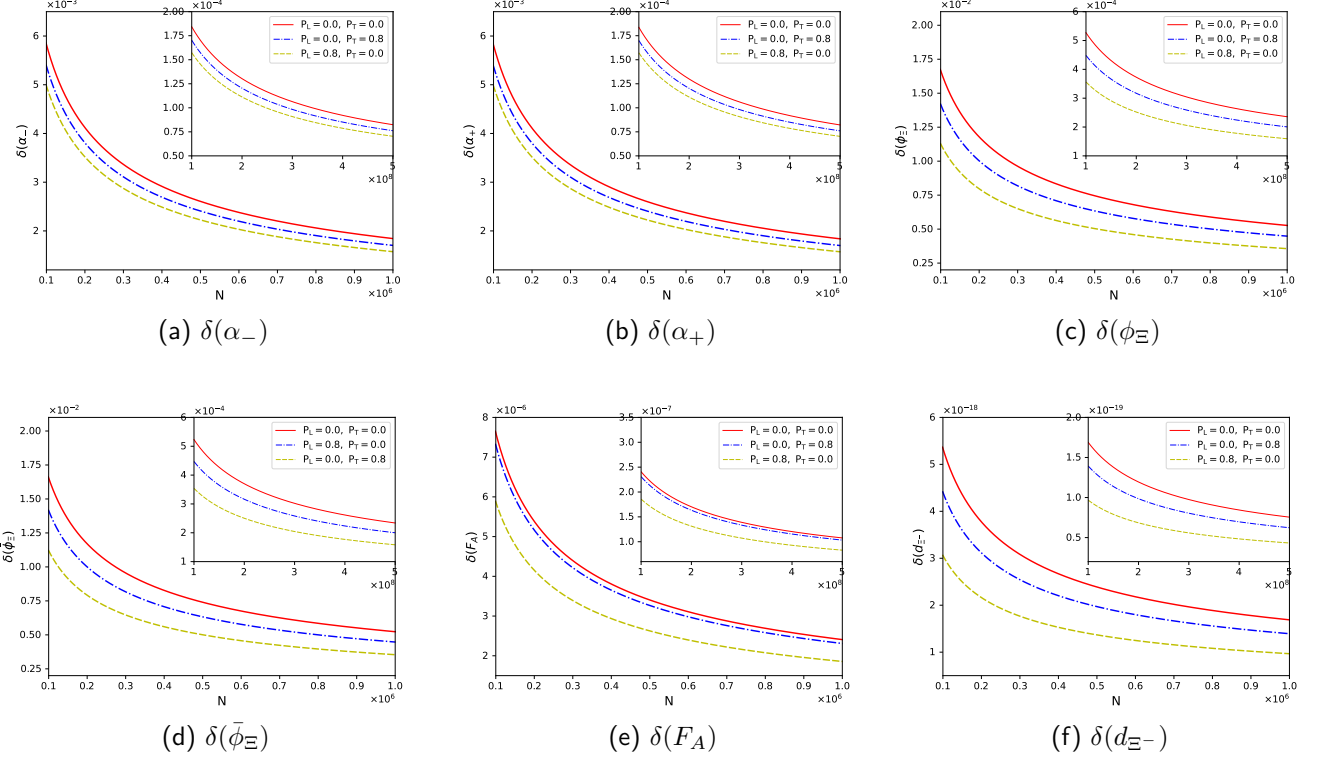


FIG. 7: Sensitivities for decay parameters (a) α_- , (b) α_+ , (c) ϕ_Ξ and (d) $\bar{\phi}_\Xi$, (e) P-violating term F_A , and (d) electric dipole moment d_{Ξ^-} in $J/\psi \rightarrow \Xi^- (\rightarrow \Lambda\pi^-)\bar{\Xi}^+ (\rightarrow \bar{\Lambda}\pi^+)$ decays.

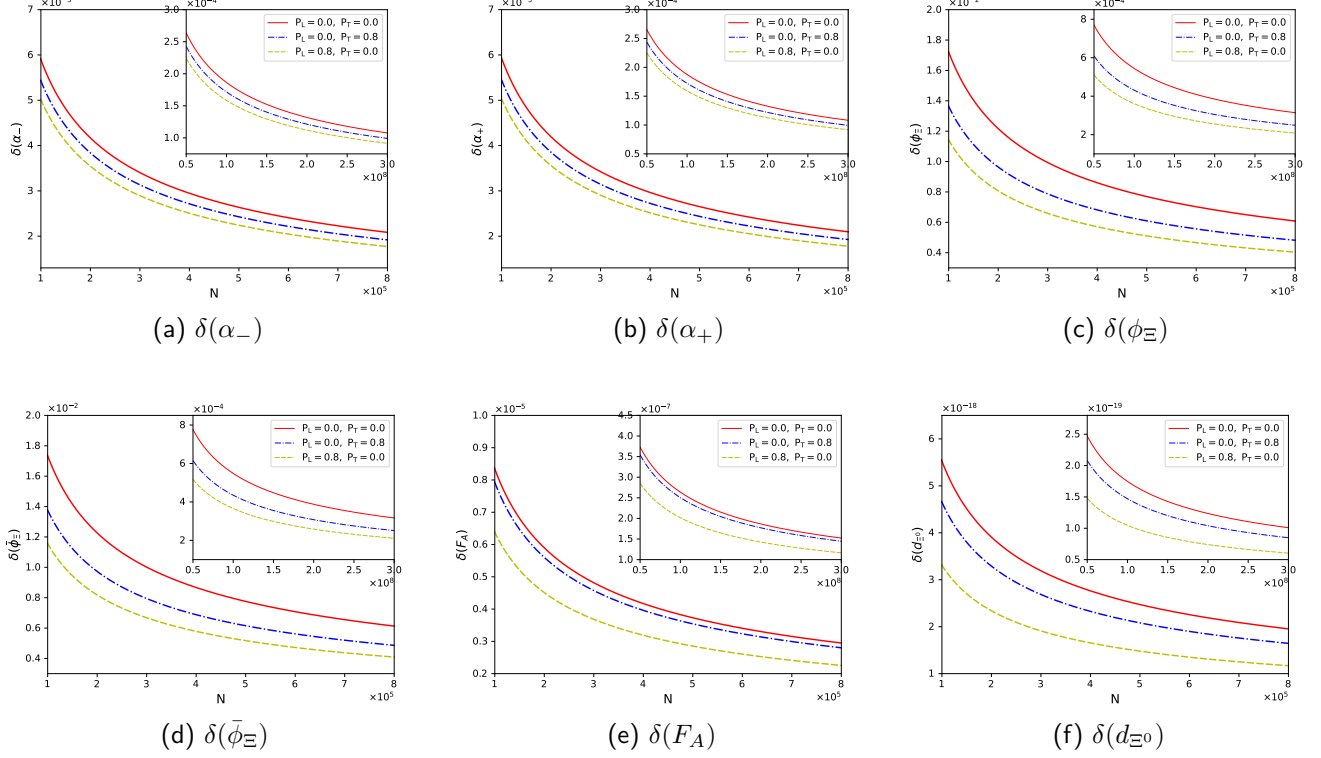


FIG. 8: Sensitivities for decay parameters (a) α_- , (b) α_+ , (c) ϕ_Ξ and (d) $\bar{\phi}_\Xi$, (e) P-violating term F_A , and (d) electric dipole moment d_{Ξ^0} in $J/\psi \rightarrow \Xi^0 (\rightarrow \Lambda\pi^0)\bar{\Xi}^0 (\rightarrow \Lambda\pi^0)$ decays.